Journal of Non-Crystalline Solids 486 (2018) 19–26

Contents lists available at ScienceDirect

Journal of Non-Crystalline Solids

journal homepage: www.elsevier.com/locate/jnoncrysol

Detailed study about the thermal behavior and kinetics characterization of an oxyfluoride tellurite glass

N. Elkhoshkhany*, Eslam Syala

Department of Material Science, Institute of Graduate Studies and Researches, 163 Horreya Avenue, Shatby, 21526, Alexandria University, Egypt

ARTICLE INFO

Keywords:
Oxyfluoride glass
TeO_2
Thermal
Kinetics

ABSTRACT

As a continuation of the earlier work (synthesis and optical properties of new fluoro-tellurite glass within (TeO_2–ZnO–LiF–Nb_2O_5–NaF) system), the thermal behavior and kinetics characterization of the oxyfluoride tellurite system have been achieved as a function of growing the mol% of NaF. The differential scanning calorimetry (DSC) technique at various heating rates under the non-isochronal conditions was used to identify the characteristic temperatures like the glass transition (*Tg*), the softening (*Ts*), the crystallization (*Tc*), the liquidus (T_L), and the melting (*Tm*) of the system. The glass stability and glass forming ability (GFA) parameters were determined based on these characteristic temperatures. The activation energies of both the glass transition (*Eg*) and crystallization (*Ec*) have been computed by different methods. The Avrami kinetic constant (*n*) has been determined by more than a method to identify the crystallization succession.

1. Introduction

Rather than the silicate-based glasses, the tellurite-based glasses are considered to be better host materials for fluorides [1]. This priority mainly comes from the superior optical properties of the tellurite glasses as well as the stability of the formed oxyfluoride tellurite glass which essentially ascribed to the positive role of oxygen on the glass-forming ability although its low packing (≈60%) with respect to the fluorine packing [2–5]. These glasses can find specific applications in the integrated optics such as lasers and optical waveguide amplifiers due to their low phonon energy, and high transparency (even in an infra-red region) [1,6–8]. In general, the addition of fluorides to the oxides based glasses decrease both the non-radiative loss [9] and the glass thermal stability while increase both the emission intensity [6] and fluorescence lifetimes of the glasses [10] but as a matter of specialization the addition of NaF retards both the thermal, mechanical properties and increases the corrosion susceptibility [11,12]. On the other hand, the insertion of LiF increases the electrical conductivity of the glass because of the combined action of both the lithium and fluorine ions [2,13]. Kinetics characterization of the oxyfluoride glasses is an important parameter in its processing and hence its applications [1,8]. The activation energy and the order of crystallization are the essential parameters used to characterize the glass kinetics [14]. The Differential Scanning Calorimetry (DSC) technique is a thermo-analytical method that used to study the kinetics characterization of the glass. Applying the DSC test under the non-isochronal conditions is preferable wherein this method; the sample is heated under constant heating rate while the released heat is recorded as a function of the temperature. The method is characterized by its simplicity and accuracy rather than the isothermal technique. Also, application of the DSC measurement using several heating rates yields several crystallization responses [15,16].

This article aims mainly to determine and discuss the thermal behavior and to characterize the kinetics of the present oxyfluoride tellurite glass as a function of increasing NaF content. The results of the present research should be added to become a new resource about the kinetics characterization of the oxyfluoride tellurite glasses which has not been discussed extensively earlier.

2. Experimental procedure

The existing glasses were prepared with respect to the molar composition (75TeO_2–10ZnO–5LiF–(10–x) Nb_2O_5–x NaF) where x ranges from 0 to 10 mol% and abbreviated as (TZLNN) as the following:

TZLNN1: 75TeO_2 –10ZnO –5LiF –10Nb_2O_5 - 0NaF
TZLNN2: 75TeO_2 –10ZnO –5LiF –8Nb_2O_5 - 2NaF
TZLNN3: 75TeO_2 –10ZnO –5LiF –6Nb_2O_5 - 4NaF
TZLNN4: 75TeO_2 –10ZnO –5LiF –4Nb_2O_5 - 6NaF
TZLNN5: 75TeO_2 –10ZnO –5LiF –2Nb_2O_5 - 8NaF
TZLNN6: 75TeO_2 –10ZnO –5LiF –0Nb_2O_5 - 10NaF

Details of the glass preparation, characterization by the X-ray powder diffraction (XRD), Fourier-transform-infrared (FTIR) and

* Corresponding author.
E-mail address: Elkhoshkhany@alexu.edu.eg (N. Elkhoshkhany).

https://doi.org/10.1016/j.jnoncrysol.2018.02.008
Received 12 December 2017; Received in revised form 31 January 2018; Accepted 10 February 2018

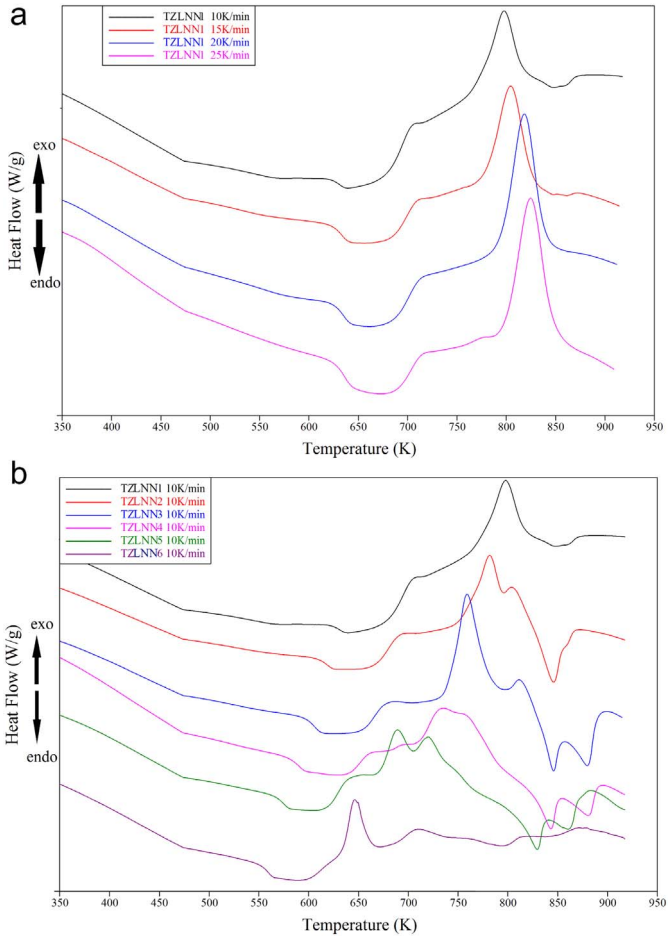

Fig. 1. The typical DSC thermograms of (a) TZLNN 1 glass at heating rates 10, 15, 20 and 25 K/min (b) TZLNN glasses at heating rate 10 K/min.

Raman spectroscopy and values of the measurements which are needed for the continuation of the work (like density and molar volume values) are found in Ref [17]. For the kinetics characterization purpose, the thermal attitude of the glass was expanding determined by the Differential Scanning Calorimetry (DSC) technique under non-isothermal (isochronal) conditions at the heating rates (β) 10,15, 20 and 25 K/min to identify the characteristic temperatures like the glass transition, softening, onset of crystallization, crystallization, liquidus and melting temperatures. The DSC test was performed via (TA Instruments, SDT Q600) and by using 14 ± 4 mg of the powdered samples in an open platinum pan with accuracy of ± 1 K in a high purity nitrogen environment with a flow rate of 15 pound per square inch (Psi) at temperature up to ≈930 K starting from room temperature. TA Instruments Universal Analysis 2000 program was used to determine all the characteristic temperatures from the DSC charts.

3. Results and discussion

Fig. 1(a and b) indicates the DSC profiles of the synthesized TZLNN glasses where Fig. 1(a) is for TZLNN1 glass at the 10, 15, 20 and 25 K/min heating rates and Fig. 1(b) represents the entire TZLNN samples at 10 K/min heating rate. Each DSC curve is found to divide to the following zones: the first endothermic dip represents the glass transition which represented by the temperature (*Tg*) and which is followed by exothermic rise due to the softening temperature (*Ts*) [18]. The strong exothermic peak is corresponding to the crystallization process which has the onset temperature (*Tx*) and the maximum peak temperature (*Tc*). The final endothermic peak represents the complete melting of all phases formed within each sample. The onset of this peak indicates the liquidus temperature of systems (T_L) [19] while its maximum refers to the melting temperature of the system (*Tm*). The phenomena of both the softening and melting (thus the liquidus) with respect to TZLNN6 glass and TZLNN1, TZLNN2 glasses respectively are absent as shown in the profiles in Fig. 1. All the characteristic temperatures are collected in Table 1. The quantitative analysis of the thermal behavior of the glass requires calculation of some moduli (i.e.) the mean cross-link density per unit formula ($\bar{n}_c$), the average stretching force of the bond ($\bar{F}$), and number of bonds per the unit volume (n_b) [20].

Firstly, the average cross-links per unit formula ($\bar{n}_c$) can be

Table 1
The glass transition temperature (*Tg*), softening temperature (*Ts*), starting of the crystallization temperature (*Tx*), maximum crystallization temperature (*Tc*), liquidus temperature (T_L), and the melting temperature (*Tm*) of TZLNN glasses.

Sample	Heating rate (β) (K/min)	*Tg* ± 1 (K)	⟨*Tg*⟩	*Ts* ± 1 (K)	⟨*Ts*⟩	*Tx* ± 1 (K)	⟨*Tx*⟩	*Tc* ± 1 (K)	⟨*Tc*⟩	T_L ± 1 (K)	⟨T_L⟩	*Tm* ± (K)	⟨*Tm*⟩
TZLNN1	10	621.80	622.63	705.90	711.04	771.00	786.51	797.80	810.39	–	–	–	–
	15	622.00		709.78		780.22		804.91		–		–	
	20	621.72		713.40		794.52		814.87		–		–	
	25	625.00		715.10		800.31		824.00		–		–	
TZLNN2	10	608.68	611.80	692.41	697.44	759.10	762.51	781.63	793.10	–	–	–	–
	15	611.73		694.29		757.00		782.17		–		–	
	20	610.45		699.39		766.00		794.61		–		–	
	25	616.35		703.70		767.94		814.00		–		–	
TZLNN3	10	594.40	596.88	680.08	682.40	740.58	744.89	754.00	762.06	861.75	862.52	880.53	880.52
	15	595.66		678.46		742.00		755.20		859.54		880.10	
	20	595.91		684.28		746.00		768.10		856.42		880.78	
	25	601.56		686.80		751.00		770.95		872.40		880.70	
TZLNN4	10	583.15	588.48	669.07	671.70	713.00	726.38	729.90	745.93	860.30	861.94	881.39	881.53
	15	588.23		671.95		727.00		745.90		861.81		881.23	
	20	590.34		672.90		732.54		753.19		862.25		881.81	
	25	592.20		672.90		733.00		754.73		863.42		881.72	
TZLNN5	10	563.72	566.64	639.66	649.59	672.03	682.24	688.70	703.21	843.57	854.22	861.72	868.55
	15	565.20		652.00		681.00		699.70		846.66		858.52	
	20	566.30		653.28		686.54		714.30		866.20		879.61	
	25	571.34		653.43		689.42		710.14		860.46		874.35	
TZLNN6	10	548.34	552.23	–	–	635.12	638.28	644.90	654.07	811.27	819.74	844.80	850.53
	15	550.03		–		636.00		646.30		828.00		849.03	
	20	554.80		–		641.00		662.48		815.36		853.71	
	25	555.77		–		641.00		662.62		824.36		854.61	